Hindawi
Mathematical Problems in Engineering
Volume 2022, Article ID 9171300, 15 pages
https://doi.org/10.1155/2022/9171300

Research Article

Flexural Reinforcement of Over-Reinforced Beam by Ultrahigh Performance Concrete Layer

Yang Song,[1,2] Shuwen Yao,[2] and Long Liu[2]

[1]*School of Architectural Engineering, The Open University of Henan, Zhengzhou 450008, China*
[2]*Anyang Engineering Research Center of High Ductility Concrete Structure, Anyang Institute of Technology, Anyang 455000, China*

Correspondence should be addressed to Long Liu; 20160913@ayit.edu.cn

Received 4 November 2022; Revised 23 November 2022; Accepted 2 December 2022; Published 23 December 2022

Academic Editor: Jan Vorel

In order to improve the failure state of over-reinforced beams and enhance their ductility, an innovative reinforcement method was proposed by adding an ultrahigh performance concrete (UHPC) layer on the top surface of the over-reinforced beam to take advantage of the high compressive strength of UHPC. The numerical simulation method was used to carry out the research. The validity of the finite element model was verified by comparing it with the experimental results, and the effectiveness of the new reinforcement method was verified by comparing it with the calculation results after adding the UHPC layer. Then, a detailed parameter study was carried out, including the thickness of the UHPC layer, the cross-section area of longitudinal tension rebar, and concrete strength. The load-deflection curve, flexural bearing capacity, and deflection ductility coefficient were studied. The results show that the bearing capacity of the UHPC-reinforced over-reinforced beams is significantly increased by 88.1%. And the stiffness and ductility of the beams are also significantly increased, with the ductility coefficient reaching 23.85. In addition, flexural bearing capacity increases with the thickness of the UHPC layer and sectional area of longitudinal tension rebar. Finally, a prediction model for the flexural bearing capacity of UHPC layer-reinforced over-reinforced beams is proposed, which further verifies the effectiveness of this method.

1. Introduction

In recent years, the need for structural reinforcement has increased dramatically, which is mainly to overcome structural aging, disaster-related structural damage, and degradation of material properties, or to improve the capacity of structures to withstand greater loads. Reinforcement techniques commonly used in tension and compression zones of reinforced concrete (RC) beams, such as externally bonded steel plates [1] and fiber-reinforced polymer (FRP) laminates [2], have been studied extensively. There are some disadvantages of the external bonded steel plate reinforcement method, such as difficulty in carrying heavy steel plate, shear failure of reinforced beam, and corrosion of steel plate. At the same time, the FRP laminate reinforcement technology also has some shortcomings. For example, FRP laminates cannot be effectively compressed under cyclic loading, and the reinforced members may suffer brittle failure due to the mismatch of tensile strength and stiffness between FRP and concrete [3]. As a material with superior compressive performance, UHPC provides a feasible method for strengthening RC beams. UHPC, also known as reactive powder concrete (RPC), is an innovative cementifying material consisting of an optimized gradation of particle composition, a water-binder ratio of less than 0.25, and a high proportion of discontinuous internal fibers [4]. It has superior properties such as high compressive strength, durability, and long-term stability [5–7]. It is possible to increase the UHPC layer in the compression zone of the over-reinforced beam to improve its flexural bearing capacity and ductility.

A large number of studies have shown that UHPC is feasible to strengthen RC beams. UHPC has been widely used in highways and bridges [8, 9], roads [10], and tunnels

[11]. RC slabs have been reinforced by Yin et al. [12, 13] with UHPC, and loading experiments have been carried out. The results show that compared with the unreinforced RC slab, the RC slab with UHPC has less oblique cracks, and UHPC has good energy absorption property and extensive flexural hardening and ductility after cracking. Besides, the ultimate load increases with the increase of the thickness of the reinforced layer. Farzad [14] used the UHPC layer to reinforce RC beams and conducted an in-depth study on the performance of reinforced beams. The results showed that the UHPC layer improved the flexural bearing capacity, stiffness, and ductility of RC beams.

Fatigue experiments were conducted by Ramachandra Murthy et al. [15] on RC beams reinforced with UHPC layers and found that the use of UHPC layers could effectively strengthen and repair damaged RC beams. A finite element model was proposed to predict the number of failure cycles and load-deflection characteristics of RC beams, while the damage degree of RC beams and fracture behavior of concrete and UHPC were considered. The results show that the UHPC layer has great potential in strengthening the bridge deck under cyclic loading. In conclusion, UHPC, as an innovative high compressive material, can be used to strengthen or repair RC beams. It not only enhances the crack resistance and flexural bearing capacity of RC beams but also improves the permeability and durability of RC beams and prolongs their service life.

Too much longitudinal tension rebar will increase the possibility of brittle failure of RC beams. Before the rebar yields, concrete in the compression zone is broken prematurely, which leads to the sudden failure of the section. At this time, the deflection and crack of the beam are small, and this failure mode is not desirable. In addition, when the over-reinforced beam is destroyed, the tension rebar does not reach the yield strength. Although this kind of beam has many rebars, it cannot give full play to their tensile strength. Accordingly, over-reinforced beams are undesirable in practice [16]. However, over-reinforced beams may be used when the height of beams is limited due to the needs of building functions. In addition, over-reinforced beams may occur when the strength of concrete decreases over time, or when the strength of poured concrete does not meet design requirements. In order to avoid brittle compression failure, the research of over-reinforced beams mainly focuses on setting external constraints or adding compression layers in the compression zone. The external constraints mainly include the use of steel and other materials to constrain the compression of concrete. At present, many researches restrict the compression zone of beams in the form of spiral rebar or stirrups. Hadi and Elbasha [17] made experiments on 10 beams constrained by spiral rebar to study the ductility of beams with spiral rebar applied in the compression zone. The results showed that the deflection ductility coefficient of beams constrained by spiral rebar was larger, and the deflection ductility coefficient increased as the pitch decreased. Whitehead and Ibell [18] placed spiral bars in the compression zone of over-reinforced beams and conducted experimental researches. The results showed that a large ductility would be obtained by using this method, and brittle failure caused by a large proportion of tension rebar would be avoided by using constraints in the compression zone of the beam. Mohamed [19] made experiments by setting constraints in the compression zone of over-reinforced beams. The results showed that the ductility of RC beams could be improved by using rectangular tension bars to constrain the compression zone, and the spiral constraint was more effective than the rectangular constraint. Priastiwi et al. [20] set additional constraint stirrups in the compression zone of concrete beams, which improved flexural bearing capacity and ductility significantly compared with the control beams. The method of adding the UHPC layer in the compression zone of over-reinforced beams has not been reported in the current research. Therefore, it is of great value to verify its feasibility theoretically.

Workforce and material resources are often consumed in the experiments of reinforced concrete components. Using a reasonable finite element model to analyze and predict the performance of concrete components can solve the problems of time-consuming, expensive, and consuming workforce. Fahiminia and Shishegaran [21] simulated and presented computational fluid dynamics (CFD) models and formulas in their experiments on viscous dampers and evaluated the validation of numerical and computational models. They also accurately analyzed the seismic performance of building components with and without viscous dampers. Shishegaran et al. [22] used ultrasonic pulse velocity (UPV) and rebound number (RN) to predict the mixed model of concrete compressive strength. Bigdeli et al. [23] used nonlinear finite element analysis and alternative models to evaluate the performance of reinforced concrete tunnels (RCT) under internal water pressure. The finite element model is also widely used in studying the flexural behavior of reinforced concrete beams. A suitable finite element model can also simulate the mechanical behavior of RC beams. Shishegaran et al. [24] carried out finite element analysis on reinforced concrete members, evaluated the flexural capacity, ductility, strength, and cracking zone, and compared it with the traditional model. The finite element simulation and experimental test results showed that the proposed system had a significant impact on improving the bearing capacity and stiffness of RC beams. In addition, he verified the validity of the finite element model by comparing the load-deflection results obtained from finite element analysis and experimental tests with the observed cracks in his research on improving the flexural ability of concrete beams. Based on the verified finite element model, the stress distribution on ordinary and TSS rebars was evaluated [23, 25, 26]. The finite element model of UHPC-RC composite slabs was established by Zhu et al. [27] with ABAQUS, and at the same time, geometric discontinuous cracks were introduced on this basis. Meanwhile, the UHPC-RC interface model was introduced into the finite element model based on the study of the bond strength between UHPC and concrete. The finite element model results are in good agreement with the experimental results, which verifies that the interface model has a good accuracy in finite element simulation. Yuan et al. [28] proposed a finite element modeling method for UHPC-NC composite components,

which considered the fracture and softening behaviors of UHPC and NC as well as their interface contact. In ABAQUS software, user subroutines UEL and UMAT were used to simulate UHPC-NC composite components, and damage experiments were carried out as well as comparison between finite element simulation results and experimental results. The results showed the finite element modeling method could truly reflect the damage mode and load-deflection curve of unreinforced UHPC-NC composite members. In conclusion, the finite element model can be used as an effective tool to make the evaluation of ultimate bearing capacity and failure state of reinforced RC beams.

The first novelty of this study is based on the high compressive strength, durability, and long-term stability of UHPC, using the UHPC layer to strengthen the over-reinforced beam to change its brittle failure state and improve its ductility. The second novelty is to simulate the mechanical properties of RC beam and UHPC layer reinforced RC beams and analyze the changes in the bearing capacity and ductility of the reinforced beams. The reinforcement method is shown in Figure 1. The finite element model of the RC beam was established, and the finite element model results were compared with the experimental results in the literature [29]. The rationality of the finite element model was verified by comparison of the load-deflection curve, crack distribution, and failure modes, which is a common research method [30, 31]. A more detailed study was carried out on the parameters of the new reinforcement method later, including the thickness of the UHPC layer, the cross-section area of longitudinal tension rebar, and concrete strength. Finally, a prediction model of the flexural bearing capacity of UHPC layer reinforced over-reinforced beams was proposed, and the predicted flexural bearing capacity of the model is in good agreement with the finite element model.

2. Methods

2.1. Experiment Overview. The basic information of the experimental beam in this study is shown in Table 1. Two 22 mm diameter steel bars are arranged at the bottom of the section, and four 10 mm diameter steel bars are used in the top compression zone. The 8 mm diameter stirrups are placed at 80 mm intervals in the shear span. The thickness of the concrete protective layer is 20 mm. Shear connectors are set at the interface between the RC beam and UHPC layer, with a depth of 60 mm and a spacing of 250 mm, to ensure that the performance of the reinforced material is fully utilized, which conforms to the requirements of GB50017-2003 [32]. Namely, the depth of the shear connector shall not be less than four times the diameter of the shear connector. Four-point loading scheme is adopted in experiments, the distance between the two loading points is 400 mm, and the net span of the beam is 1700 mm, as shown in Figure 2.

Among the 11 beams, 10 are UHPC layer reinforced beams, and 1 is unreinforced control beam. In addition, variable parameters include (a) thickness of the UHPC layer, (b) sectional area of longitudinal tension rebar, and (c) concrete. Table 1 shows the specific parameters of the experimental beam. The meaning of UB30-20-24 is as follows: UB represents RC beams reinforced with UHPC layer, 30 represents the thickness of UHPC layer which is 30 mm, 20 represents the diameter of tensile longitudinal rebar which is 20 mm, and 24 represents the strength of concrete which is 24 MPa. CB-2 is an unreinforced beam.

2.2. Finite Element Model. In this study, ABAQUS is adopted to simulate the experimental beam, which will make reflections of the nonlinear behavior of the material accurately. It is assumed that there is no bond slip between rebar and concrete as well as UHPC layer and concrete. In order to avoid stress concentration, rigid pads are set at the support and loading point, respectively.

C3D8R solid element is used to simulate concrete, UHPC layer, pad, and studs, and T3D2 element is used to simulate steel bars. The binding constraint is adopted between plates and the beams, the internal area contact is used between steel bars and the concrete beams, and UHPC layers and the RC beams are connected by the bolts. At the same time, the "tractor-separation model" is used to simulate the contact between UHPC layers and beams. Simply supported constraints are adopted in experimental beams, that is, the displacement degrees of freedom $U1$, $U2$, and $U3 = 0$ are set at the left end, the rotational degrees of freedom UR2 and UR3 = 0, and the displacement degrees of freedom $U1$ and $U2 = 0$ are set at the right end, the rotational degrees of freedom UR2 and UR3 = 0. The "Tie" method is used to simulate the interaction between beam and pad, and the "Embedment" method is used to simulate the interaction between beam, rebar, and bolt. The mesh size of the finite element model is 40×40 mm [30, 31]. The finite element model is shown in Figure 3.

2.2.1. Concrete. In ABAQUS, there are two main methods for concrete simulation, namely, concrete dispersion cracking model and concrete plastic damage (CDP) model [33]. Different from the dispersion cracking model, which is only used for dynamic load analysis, the CDP model can be used to simulate the mechanical behavior of concrete under static and dynamic loads. Lee et al. [34] made conductions of finite element analysis on RC beams with ABAQUS. He assumed that the rebar and concrete were perfectly bonded, and the tension damage form of concrete obtained from the finite element model was similar to the crack form in the experiment. Meanwhile, ultimate strength, deformation, and stress obtained by the finite element model were in good agreement with the measured values. In addition, the CDP model does not give rise to convergence problems. The use of CDP in the modeling process requires the determination of a set of parameters to capture the mechanical behavior of concrete accurately, and the values of these parameters are from the ABAQUS manual [35]. The simulation results obtained by Raza et al. [36] using these parameters are in good agreement with experimental results, and these parameters are also used in this study, as shown in Table 2. The mechanical properties of concrete are shown in Table 3.

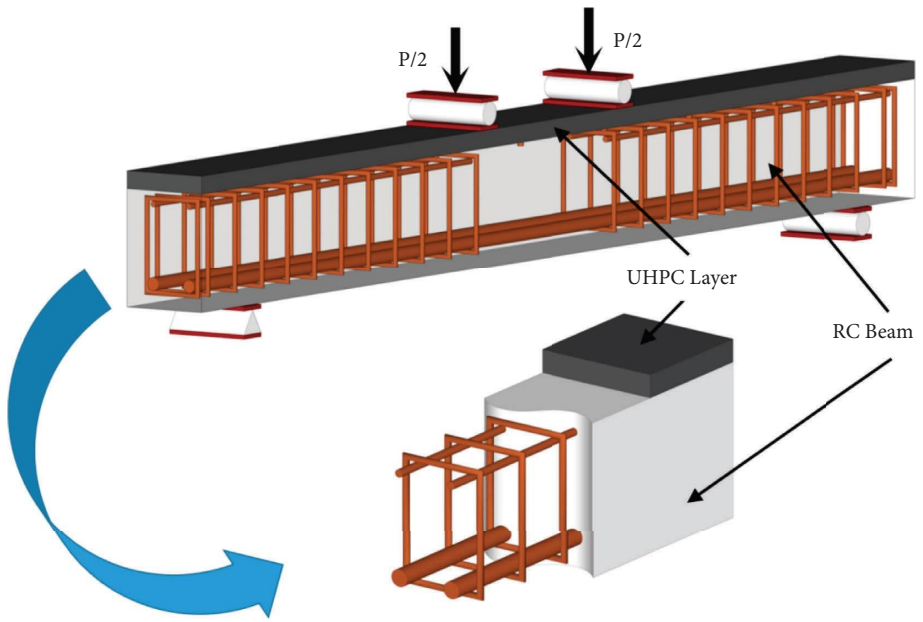

Figure 1: Schematic diagram of UHPC layer reinforced over-reinforced beam.

Table 1: Parameters of the experimental beam.

Beam	Diameter of longitudinal tension rebar (mm)	Thickness of UHPC layer (mm)	Strength of concrete (MPa)
CB-2	22	—	24
UB30-20-24	20	30	24
UB30-22-24	22	30	24
UB30-25-24	25	30	24
UB30-28-24	28	30	24
UB40-22-24	22	40	24
UB50-22-24	22	50	24
UB60-22-24	22	60	24
UB70-22-24	22	70	24
UB30-22-29	22	30	29
UB30-22-34	22	30	34

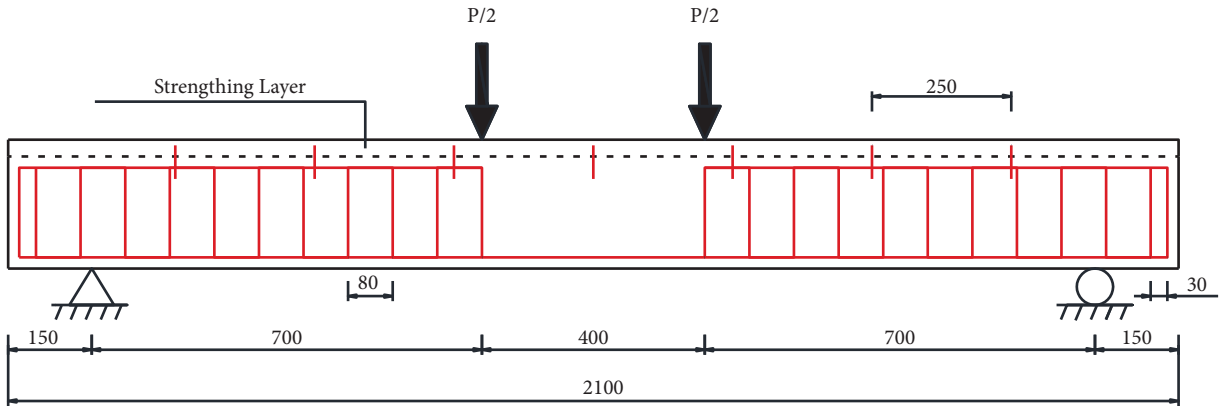

(a)

Figure 2: Continued.

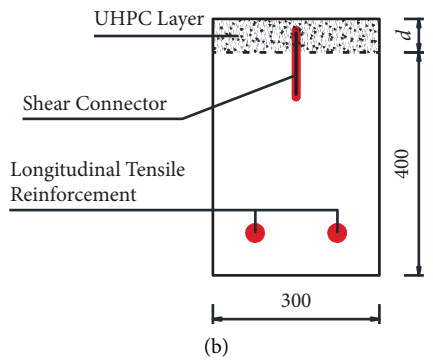

Figure 2: Schematic diagram of experimental beam size: (a) elevation; (b) sectional view.

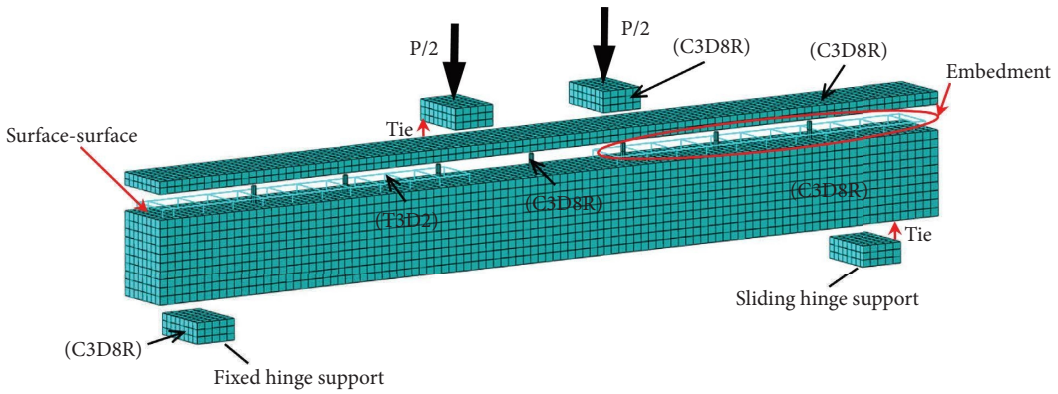

Figure 3: Schematic diagram of finite element model.

Table 2: Plastic damage model parameters.

Parameters	Values
Expansion angle	30°
Eccentricity	0.1
f_{b0}/f_{c0}	1.16
K	0.667
Viscosity coefficient	0.001

Concrete constitutive relation curve refers to the current GB 50010-2010 code for the design of concrete structures [37]. Figure 4 provides the constitutive relation curve, compression damage, and tension damage parameters of concrete.

2.2.2. Rebar. In this study, an elastoplastic model is used to simulate longitudinal rebar and stirrup, namely, the linear elastic behavior of rebar is defined by elastic modulus and Poisson's ratio, and the plastic behavior is defined by yield stress and plastic strain. The properties of rebar are shown in Table 4, and the stress-strain curve of rebar is shown in Figure 5.

2.2.3. UHPC. In order to obtain the constitutive relationship of UHPC, Zhang et al [38] conducted an axial tension test on UHPC specimens, the axial tension characteristic

Table 3: Mechanical properties of concrete.

Item	f_c' (MPa)	f_t (MPa)	E_c	ν
Value	24.0	2.27	31553	0.2

parameters of four kinds of UHPC with different fiber content were compared and analyzed by using the control variable method. Based on experimental results, a tensile constitutive model of UHPC was proposed. The expression of the stress-strain curve of UHPC proposed by different scholars was summarized by Prem et al. [39], the effects of different steel fiber content on the performance of UHPC were studied, the stress-strain characteristics of UHPC were evaluated, and the compressive constitutive model of UHPC was established according to the experimental data. The model can completely express the stress-strain behavior of UHPC and has a good correlation with the experimental data.

The tensile stress-strain relationship of UHPC used in this study is shown in the following formulas:

$$\sigma_{(\varepsilon)} = \frac{f_{ct}\varepsilon}{\varepsilon_{ca}} \quad 0 \le \varepsilon \le \varepsilon_{ca}, \tag{1}$$

$$\sigma_{(\varepsilon)} = f_{ct} \quad \varepsilon_{ca} \le \varepsilon \le \varepsilon_{pc}, \tag{2}$$

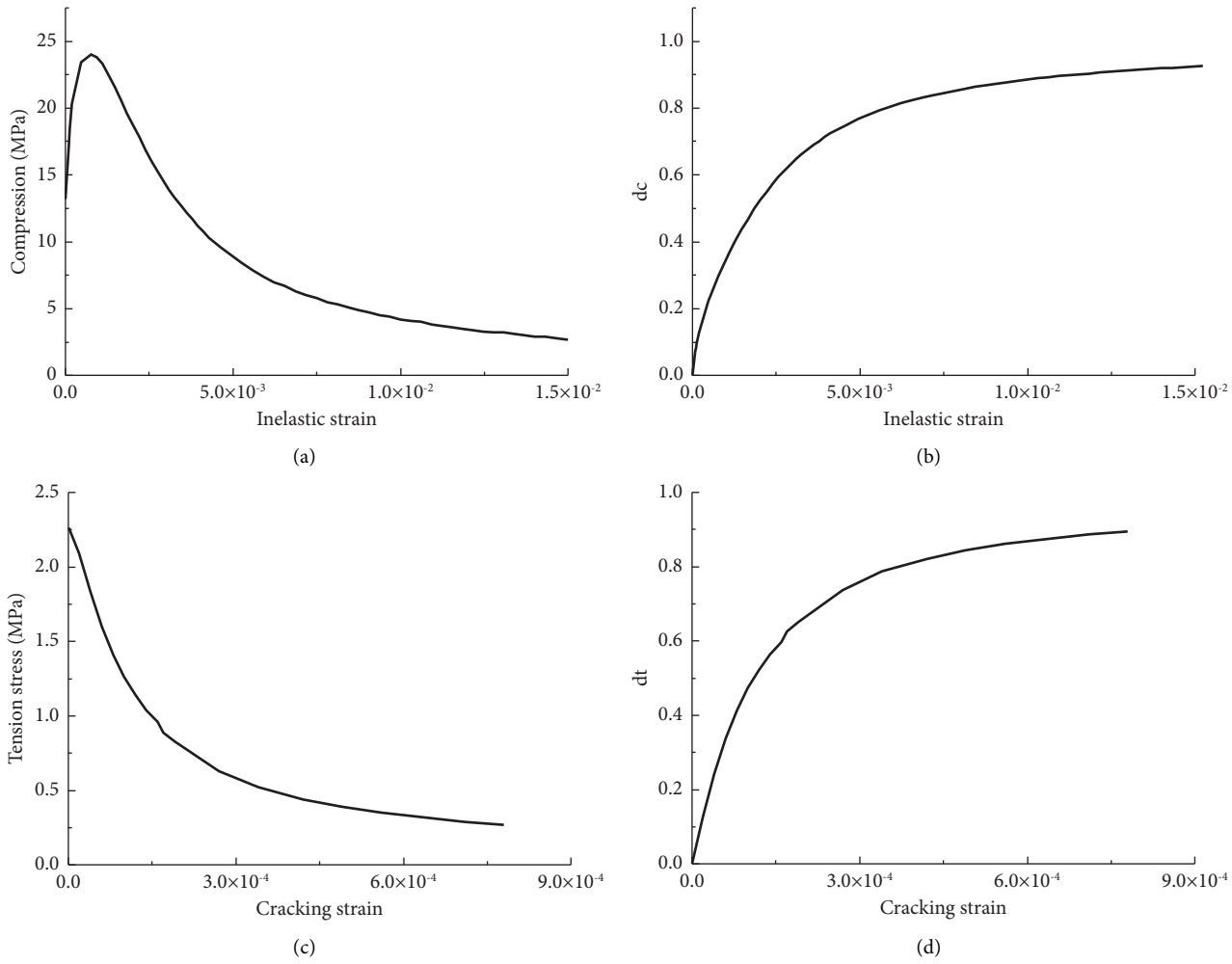

Figure 4: Constitutive relation curve of concrete: (a) compressive stress vs. inelastic strain; (b) compressive damage vs. inelastic strain; (c) tension stress vs. cracking strain; (d) tension damage vs. cracking strain.

Table 4: Mechanical properties of rebar.

Rebar	Diameter (mm)	Elasticity modulus (GPa)	Poisson's ratio	Yield strength (MPa)
Stirrup	8	200	0.3	305
Compression rebar	10	200	0.3	405
Tension rebar	20 22 25	200	0.3	405

where $\sigma_{(\varepsilon)}$ is the tensile stress of UHPC; ε is the tensile strain of UHPC; f_{ct} is the elastic ultimate tensile strength of UHPC; ε_{ca} is the elastic ultimate tensile strain of UHPC; ε_{pc} is the ultimate tensile strain of UHPC.

The tension stress-strain relationship of UHPC is shown in the following formula:

$$y = \begin{cases} Ax + (6 - 5A)x^5 + (4A - 5)x^6, & (0 \le x \le 1), \\ \dfrac{x}{\alpha(x-1)^2 + x}, & (x \ge 1), \end{cases} \tag{3}$$

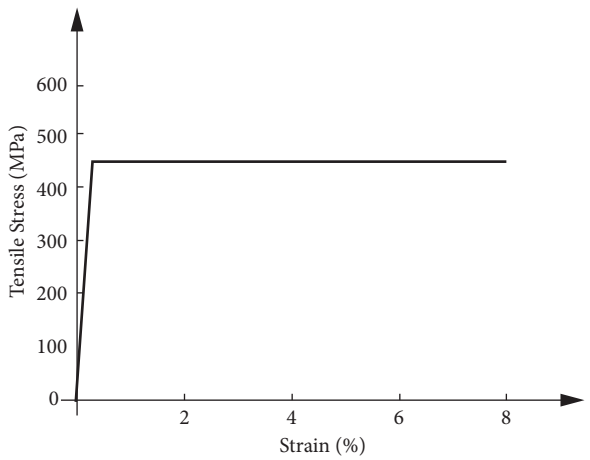

Figure 5: Stress-strain curve of rebar.

where $x = \sigma_c / f_c$ is stress of concrete under compression, f_c is axial compressive strength of prismatic body, $y = \sigma_c/\sigma_0$, σ_c is strain of concrete under compression, and σ_0 is peak compressive strain of concrete; Parameter A has clear physical significance, and it is the ratio of tangent elastic modulus E_0 at the zero point of the stress-strain curve to secant modulus E_p at the peak point.

The mechanical properties of UHPC used in this study are shown in Table 5, and the stress-strain curves of UHPC under compression and tension are shown in Figure 6.

2.2.4. Contact Interface between UHPC Layer and Concrete. There are two ways to define the contact interface between the UHPC layer and concrete, one of which was proposed by AASHTO [40] and the other by ACI [41], which specifies the minimum shear resistance at the interface of the two materials. However, the shear calculation is conservative and ignores the bond strength at the interface of concrete poured at different times. Furthermore, ACI [41] assumed that cracks have already appeared at the interface. Therefore, only the friction coefficient and shear-friction reinforcement are considered in the calculation of shear strength.

Two types of traction-separation models are available in ABAQUS to simulate interface connections. The first method uses cohesive elements of a certain thickness to simulate the contact between the UHPC layer and concrete. The other is to use surface-to-surface property settings [42, 43]. The latter is used in this study because no adhesive is added between the UHPC layer and the concrete, so the adhesive thickness can be assumed to be 0. In this study, bolts are used as the connecting member between UHPC layer and concrete, and the tractor-separation model in ABAQUS is used to simulate the interface contact between UHPC layer and concrete beam. The slip parameters of the contact surface between bolts and UHPC layer and concrete are shown in Tables 6 and 7.

2.3. Calculation Method of Yield Load. The "farthest point method" proposed by Feng et al. [44] is adopted to determine yield load on the load-deflection curve. The point farthest from the line between the origin and the peak point on the load-deflection curve is yield point, and the load at this point is yield load. If there are more than one such point, the average of these points is taken, and yield point is obtained on the load-deflection curve. As shown in Figure 7, a straight line connects the origin and the peak point, the parallel line of the line is tangent to the load-deflection curve, and the tangent point obtained is yield point.

Deflection ductility is an important mechanical property index. In this study, ductility of RC beams before and after reinforcement is analyzed, and deflection ductility coefficients are calculated according to the following formula:

$$\mu = \frac{\Delta u}{\Delta y}, \tag{4}$$

where μ is deflection ductility coefficient; Δ refers to various parameters related to deformation, such as deflection, strain, section curvature, rotation angle, or deflection; Δu is ultimate deflection; Δy is initial yield deflection.

3. Results and Discussion

3.1. Verification of the Finite Element Model. The finite element model of CB-2 was compared with the experimental results, and the correctness of finite element model was verified from the load-deflection curve, crack distribution, and failure mode.

3.1.1. Load-Deflection Curve. The finite element model established by ABAQUS simulated the whole loading process of CB-2. The comparison between the finite element model results of CB-2 and experimental results is shown in Figure 8.

As for the load-deflection curve obtained in experiment, OA is elastic working stage before cracking of CB-2. The first crack appears at the bottom of CB-2 at point A, and corresponding cracking load is 9.73 kN. AB is the working stage with cracks. The tension rebar yields at point B, corresponding yield load is 85.93 kN, and BD is the failure stage, at which the tension rebar stress remains unchanged at yield strength where BC is elastic-plastic cracking stage of CB-2. When the load reaches the peak, the upper concrete is crushed, while longitudinal tension rebar remains elastic, and the peak load at point C is 104.90 kN.

The results of the finite element model are roughly similar to experimental results with a high degree of agreement, which can also be divided into OA′ elastic working stage. The cracking load corresponding to point A′ is 15.25 kN, which is larger than experimental results. The yield load at point B′ is 86.81 kN, slightly larger than experimental result. B′D′ is failure stage, and the peak load at point C′ is 108.85 kN, which is close to experimental peak load. In addition, the slope (characteristic stiffness) of OA′ is larger than that of the experimental beam.

In general, the load-deflection curves calculated by the finite element model fit well with experimental results, indicating that the finite element model has good accuracy and applicability. In the elastic stage, the overall stiffness

Table 5: Mechanical properties of UHPC.

Elasticity modulus (GPa)	Poisson's ratio	f_c (MPa)	f_t (MPa)
48.6	0.19	144.82	8.1

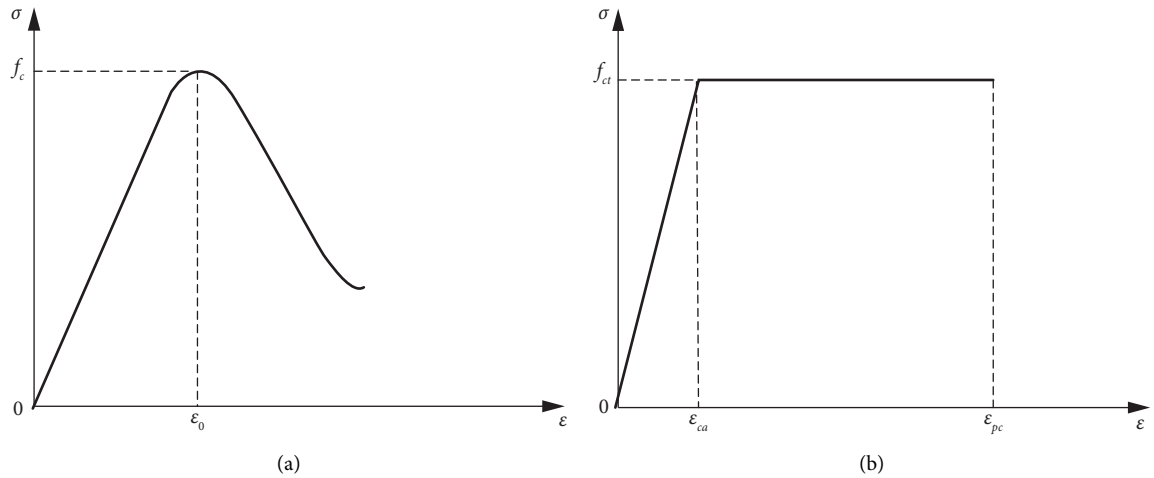

Figure 6: Stress-strain curve of UHPC: (a) compression and (b) tension.

Table 6: Mechanical properties of the study.

Elasticity modulus (GPa)	Poisson's ratio	Yield strength (MPa)
200	0.3	405

Table 7: Slip parameters of UHPC layer and concrete interface.

Parameters	Values
K_{nn} (N/mm^3)	1358
K_s, K_t (N/mm^3)	20358
t_n, t_s, t_t (MPa)	5.63
Total/plastic deflection	0.241
Viscosity coefficient	0.001
Friction coefficient	1.44

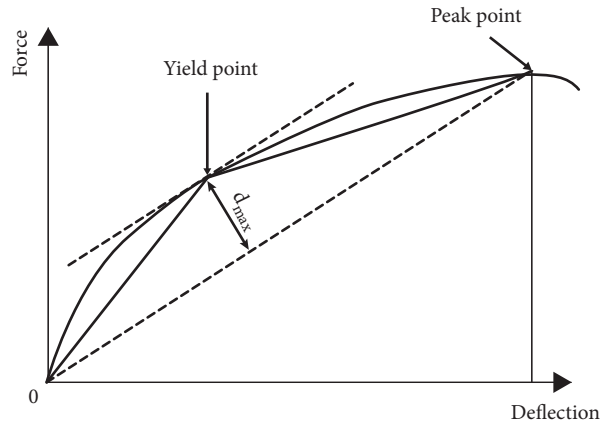

Figure 7: Schematic diagram of farthest point method.

calculated by the finite element model is higher than the experimental result. The main reasons for this deviation are as follows: (1) slight cracks occur in concrete due to shrinkage of concrete and hydration of cement, but such cracks are not considered in the finite element model; (2) the boundary conditions as strict as the finite element model cannot be achieved in the experiment; (3) the contact established in the finite element model assumes rebar and concrete are perfectly combined, and in fact, there will be bond slip between rebar and concrete in the experiment, leading to reduction of the bond between rebar and concrete.

3.1.2. Failure Mode. The finite element model can record the failure mode and crack distribution of RC beams. The failure of the experimental beam is caused by fracture of upper concrete, which is mainly related to excessive reinforcement of tensile rebar at the bottom. DAMAGET output via ABAQUS records the fracture distribution generated by this failure mode effectively. As shown in Figure 9, the fracture distribution of CB-2 in the finite element model and experiment is presented, respectively.

As can be seen from Figure 9, for CB-2, the crack distribution obtained by the finite element model and experiment is relatively consistent. At the early stage of loading, the first vertical crack appeared at the lower edge of the mid-span section. The number, width, and length of cracks increase with the increase of load. Due to the large amount of longitudinal tension rebar, when the load reaches peak, the concrete at the top of the section is crushed, but the longitudinal tension rebar still does not yield, and the beam presents brittle failure mode.

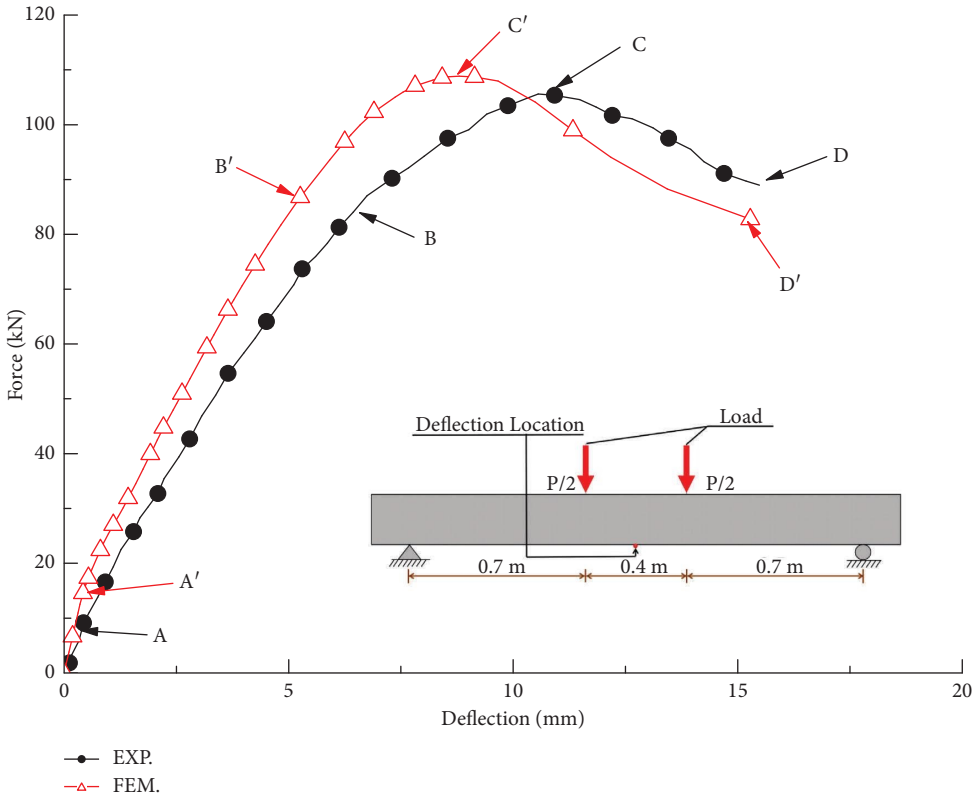

Figure 8: Load-deflection curve of CB-2.

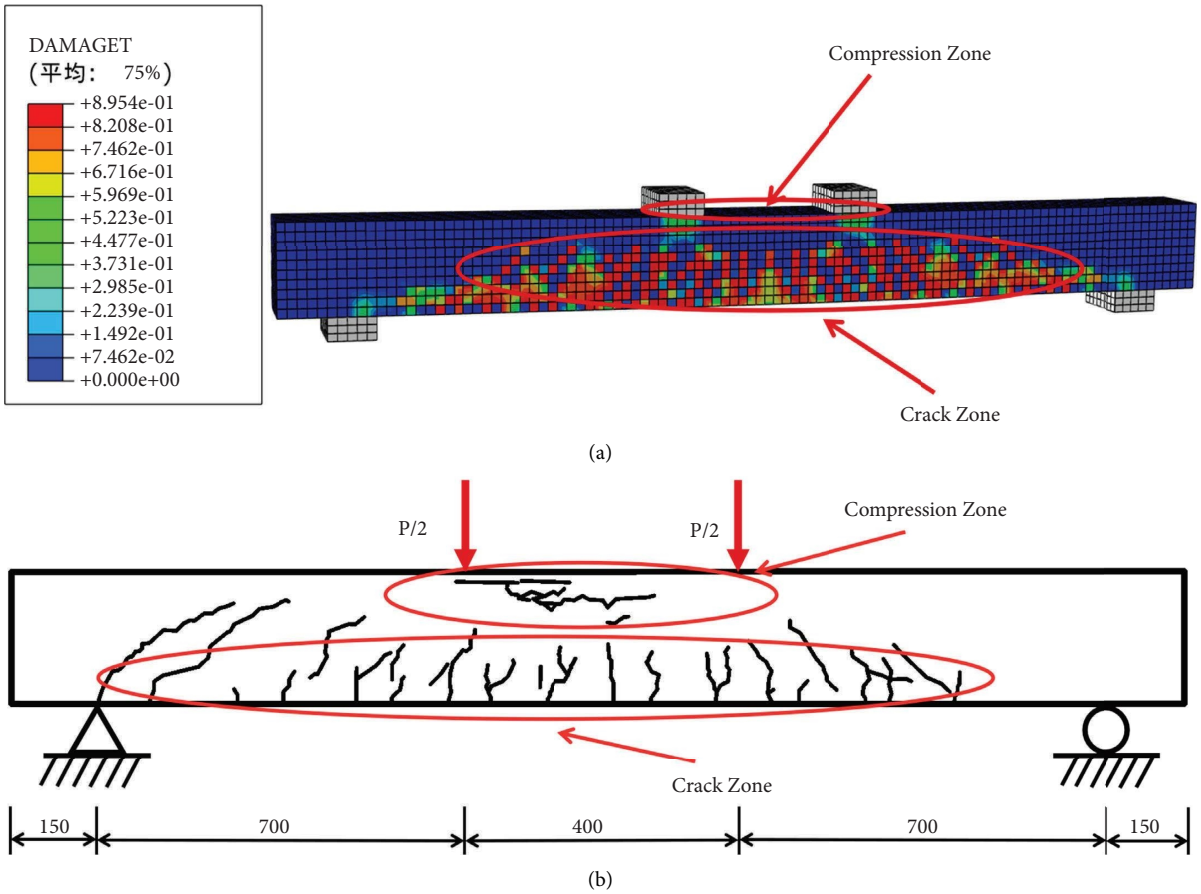

Figure 9: Crack distribution: (a) CB-2 FEM; (b) CB-2 EXP.

3.2. UHPC Layer Reinforced Over-Reinforced Beam. As CB-2 is over-reinforced beam, it shows the compressive failure of concrete in the compression zone, while longitudinal tensile rebar fails to yield. If the UHPC layer is added to the compression zone, the compressive capacity of the upper edge can be greatly improved. UB30-22-24 is obtained by adding a 30 mm thickness UHPC layer on the top of CB-2. Load-deflection curves of UB30-22-24 and CB-2 are shown in Figure 10. The influence of the UHPC layer on the flexural bearing capacity and ductility of over-reinforced beams are analyzed from the load-deflection curve, flexural bearing capacity, and ductility.

It can be seen from Figure 10 that before the first crack, the load-deflection curve of reinforced beam is almost the same as that of unreinforced beam, indicating that UHPC layer contributes little to the stiffness of RC beam before cracking. After concrete cracking at lower edge of the section, bending stiffness of the beam decreases and slope of the curve decreases, but the change is not obvious. Due to the UHPC layer being configured in the compression zone of the section, the tangent slope of the load-deflection curve of the reinforced beam after cracking is larger than that of the unreinforced beam, indicating that bending stiffness is higher than that of the unreinforced beam. And with the increase in load, the UHPC layer can still maintain a large stiffness of the beam. The load decreases obviously after reaching the peak point, and then, the load remains stable until the RC beam is destroyed after the steel bar is pulled.

Table 8 lists the main results obtained by UB30-22-24 and CB-2, including yield load, peak load, and corresponding deflection. The yield load is obtained by the "farthest point method," and the peak load is the maximum load. The deflection under yield load is Δy, the ultimate load is the value when the load drops to 85% of the peak load, and the deflection under ultimate load is Δu. The ductility coefficient of deflection is calculated according to formula (4). According to Table 8 and Figure 10, compared with CB-2, the cracking load of UB30-22-24 reinforced by the UHPC layer increases from 15.25 kN to 22.96 kN, the yield load increases from 86.81 kN to 163.26 kN, with an increase of 88.1%, and the peak load also increases from 108.85 kN to 178.76 kN. The ductility coefficient increased by 880% from 2.43 to 23.85. The results show that adding UHPC layer to the top of over-reinforced beam can significantly improve its flexural bearing capacity and ductility.

3.3. Parameter Study. In order to investigate the influence of related parameters on RC beams reinforced by UHPC layer, parameters were studied on the basis of UB30-22-24. The influences of thickness of UHPC layer, cross-section area of longitudinal tension rebar, and strength of concrete on RC beams are discussed from the aspects of load-deflection curve, flexural bearing capacity, and ductility. The load-deflection curves of reinforced beams with different parameters are shown in Figure 11.

3.3.1. Thickness of UHPC Layer. On the basis of adding UHPC layer on the top of RC beam, the influence of UHPC layer thickness on the flexural performance of over-reinforced beams is studied. Based on UB30-22-24, the thickness of UHPC layer is changed, and the thickness of UHPC layer is increased from 30 mm to 70 mm at 10 mm intervals. The load-deflection curve obtained by finite element model is shown in Figure 11(a). The load-deflection curves of reinforced beams with different thicknesses of UHPC layer coincide with each other before cracking, indicating that the change in thickness of UHPC layer has no influence on stiffness of RC beams before cracking. After the appearance of the first crack, the stiffness increases with the thickness of UHPC layer, but the change is not obvious. In addition, the change in UHPC layer thickness has an obvious influence on the flexural bearing capacity and ductility of RC beams. Yield load, peak load, and deflection ductility coefficient obtained by the finite element model are shown in Table 9.

As can be seen from Table 9, with the increase of UHPC layer thickness, the yield load of reinforced beams increases from 163.26 kN to 171.33 kN, 180.43 kN, 193.63 kN, and 201.73 kN, respectively, compared with UB30-22-24. The peak load increased from 178.76 kN to 187.97 kN, 198.84 kN, 210.36 kN, and 221.62 kN, respectively, increasing by 5.2%, 11.2%, 17.7%, and 24.0%, showing an approximate linear increase. The deflection ductility coefficient decreased from 23.85 to 19.52, 16.23, 16.24, and 15.77. However, when the thickness of UHPC layer increases from 50 mm (UB50-22-24) to 60 mm (UB60-22-24), deflection ductility coefficient hardly changes, but generally, the deflection ductility coefficient decreases with the increase of UHPC layer thickness. It can be seen that increasing the thickness of UHPC layer in a certain range will improve flexural bearing capacity of RC beams, but ductility of reinforced beams decreases. Changing the thickness of UHPC layer has a significant impact on flexural bearing capacity of RC beams.

3.3.2. Areas of Tension Rebar. Based on UB30-22-24, the influence of longitudinal tension rebar on flexural performance of over-reinforced beams is studied by changing diameter of longitudinal tension rebar. The load-deflection curve obtained by the finite element model is shown in Figure 11(b). It can be seen that the change of longitudinal tension rebar area has no obvious influence on preyield stiffness of RC beams, but it has a great influence on flexural bearing capacity and ductility. Yield load, peak load, and deflection ductility coefficient are shown in Table 10.

Compared with UB30-22-24, the cross-section area of the longitudinal tension rebar area of UB30-20-24 is slightly reduced, and the yield load of UB30-20-24 is reduced to 138.09 kN. The peak load is reduced to 152.43 kN by 14.7%. Deflection ductility coefficient increases by 2.9%. Compared with UB30-22-24, the yield loads of UB30-25-24 and UB30-28-24 increase to 209.26 kN and 218.99 kN, respectively, with the increase of the area of longitudinal tension rebar. The peak load increases to 217.74 kN and 266.62 kN, by 21.8% and 49.1%, respectively; the deflection ductility coefficient of UB30-25-24 is reduced to 14.42. It can be seen that with the increase of longitudinal tension rebar area, the yield load and peak load of the reinforced beams are greatly

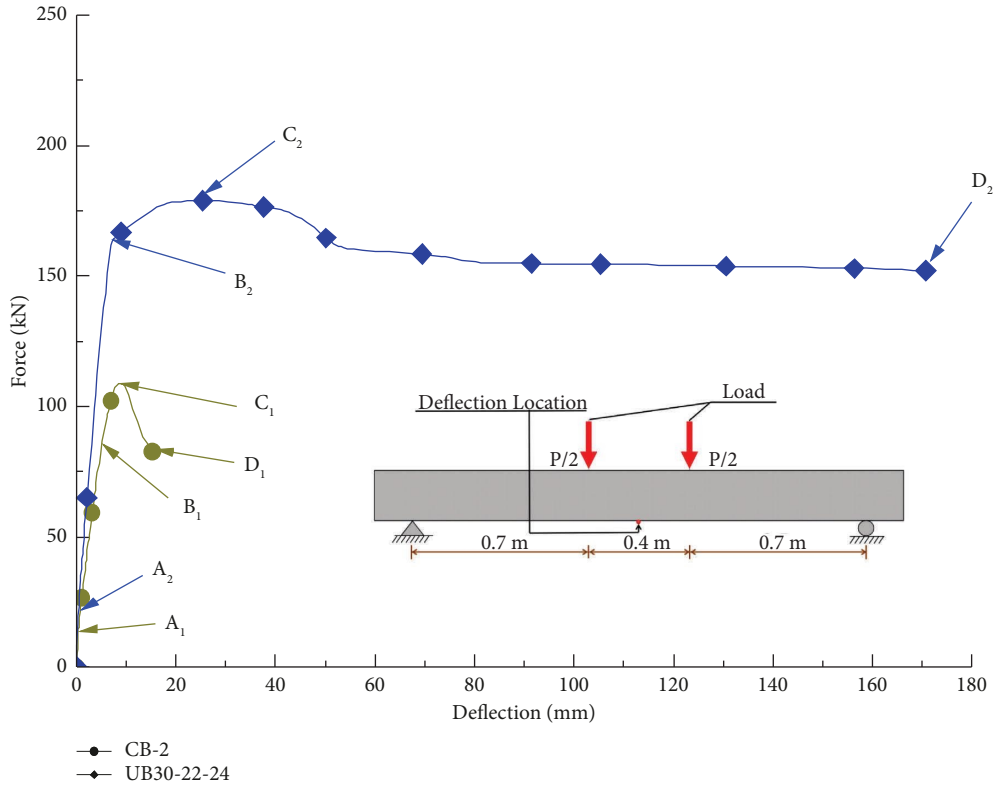

Figure 10: Load-deflection curve.

Table 8: Comparison of yield load, peak load, and ductility coefficient.

Beam	P_y/kN	P_p/kN	Peak load increment (%)	Δy (mm)	Δu (mm)	μ
CB-2	86.81	108.85	—	5.26	12.80	2.43
UB30-22-24	163.26	178.76	64.2	7.16	170.77	23.85

increased. Except UB30-28-24, the deflection ductility coefficients of the other three reinforced beams decrease successively. It shows that the flexural bearing capacity of RC beams can be improved by increasing the area of longitudinal tension rebar in a certain range, and the area of longitudinal tension rebar has a great influence on the flexural performance of RC beams.

3.3.3. Concrete Strength. Based on UB30-22-24, the influence of concrete strength on flexural bearing capacity and ductility has been studied. By increasing the concrete strength at 5 MPa intervals, UB30-22-29 with 29 MPa strength and UB30-22-34 with 34 MPa strength were obtained. The load-deflection curve obtained by the finite element model is shown in Figure 11(c). Before yielding, the load-deflection curves of the three reinforced beams coincide, indicating the change of concrete strength has no effect on the stiffness of reinforced beams, and the change law of load-deflection curves is still relatively similar after reaching yield point.

Table 11 lists the yield load, peak load, and deflection ductility coefficient for each beam. Compared with UB30-22-24, the yield load of UB30-22-29 and UB30-22-34 hardly changes. The peak load of UB30-22-29 and UB30-22-34 increases to 179.43 kN and 179.86 kN by 0.4% and 0.6%, respectively, and the deflection ductility coefficient decreases to 21.81 and 16.42. It can be seen that when concrete strength increases from 24 MPa to 34 MPa, the flexural bearing capacity of reinforced beams does not increase significantly, and the ductility coefficient of deflection decreases, indicating that increasing concrete strength cannot improve the flexural bearing capacity of reinforced beams and will also reduce the ductility.

3.4. Theoretical Analysis. The ultimate flexural bearing capacity of RC beams can be predicted according to formulas (5) and (6) for the rectangular section with single rebar. The strain and stress distributions of the section are shown in Figures 12 and 13.

$$\sum X = 0\alpha_1 f_c bx = f_y A_s, \tag{5}$$

$$M_u = \alpha_1 f_c bx\left(h_0 - \frac{x}{2}\right), \tag{6}$$

where M_u is ultimate flexural bearing capacity; α_1 is equivalent rectangular stress graphic coefficient of concrete

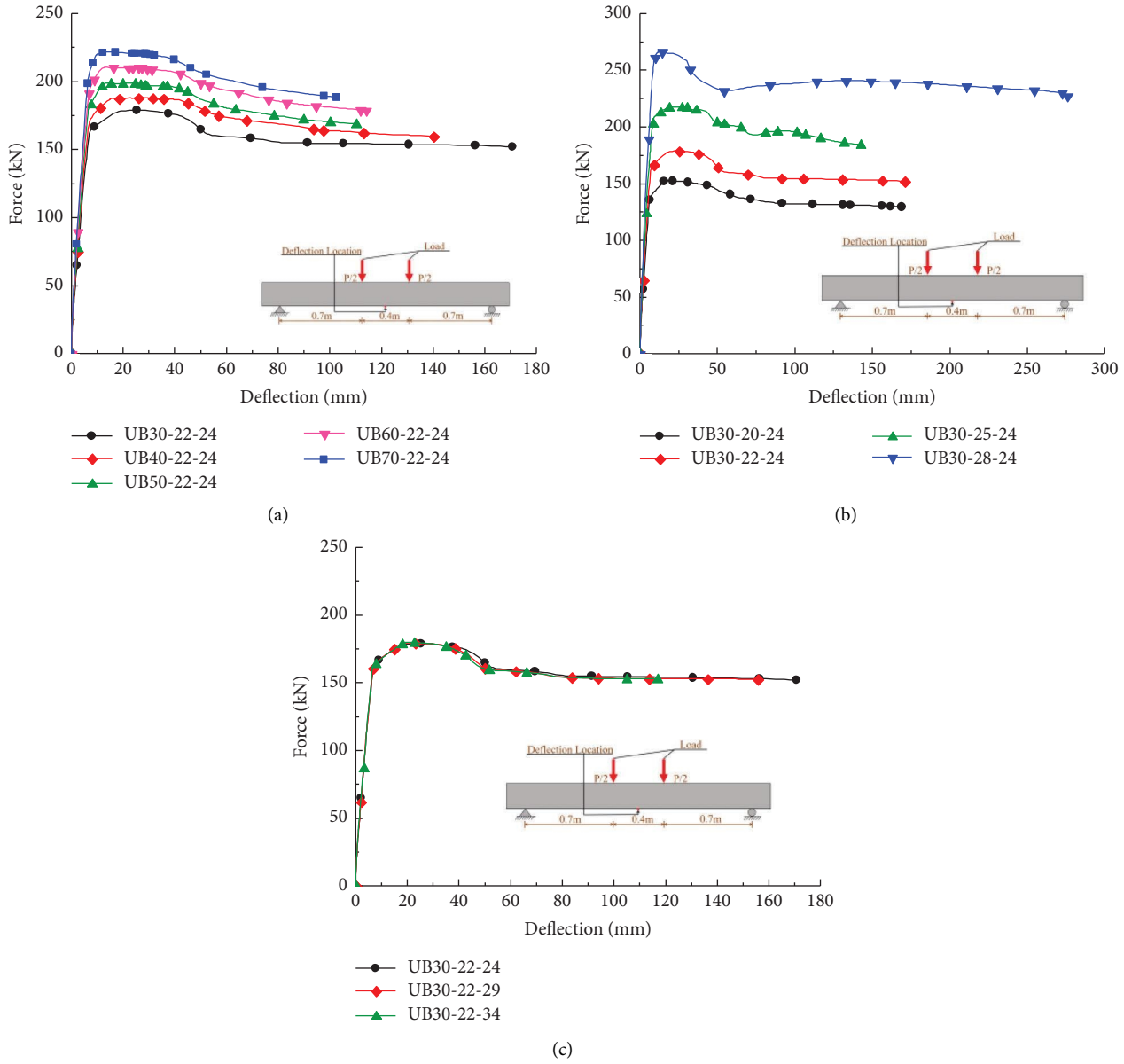

Figure 11: Load-deflection curves of reinforced beams with different parameters: (a) thickness of UHPC layer; (b) areas of tension rebar; (c) concrete strengths.

Table 9: Comparison of yield load, peak load, and ductility coefficient.

Beam	P_y/kN	P_p/kN	Peak load increment (%)	Δy (mm)	Δu (mm)	μ
UB30-22-24	163.26	178.76	—	7.16	170.77	23.85
UB40-22-24	171.33	187.97	5.2	7.18	140.13	19.52
UB50-22-24	180.43	198.84	11.2	6.70	108.72	16.23
UB60-22-24	193.63	210.36	17.7	7.02	114.02	16.24
UB70-22-24	201.73	221.62	24.0	6.51	102.69	15.77

Table 10: Comparison of yield load, peak load, and ductility coefficient.

Beam	P_y/kN	P_p/kN	Peak load increment (%)	Δy (mm)	Δu (mm)	μ
UB30-20-24	138.09	152.43	−14.7	6.89	168.98	24.53
UB30-22-24	163.26	178.76	—	7.16	170.77	23.85
UB30-25-24	209.26	217.74	21.8	9.44	136.16	14.42
UB30-28-24	218.99	266.62	49.1	6.87	276.12	40.19

Table 11: Comparison of yield load, peak load, and ductility coefficient.

Beam	P_y/kN	P_p/kN	Peak load increment (%)	Δy (mm)	Δu (mm)	μ
UB30-22-24	163.26	178.76	—	7.16	170.77	23.85
UB30-22-29	163.49	179.43	0.4	7.14	155.69	21.81
UB30-22-34	162.94	179.86	0.6	7.11	116.75	16.42

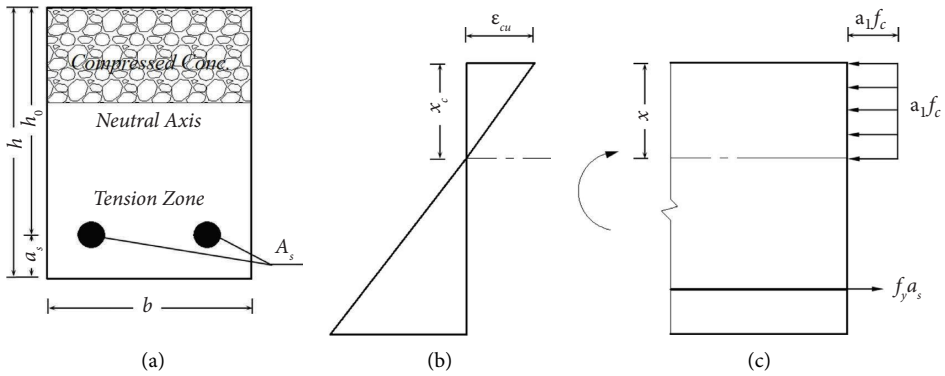

Figure 12: Strain and stress distribution: (a) section; (b) strain; (c) equivalent stress.

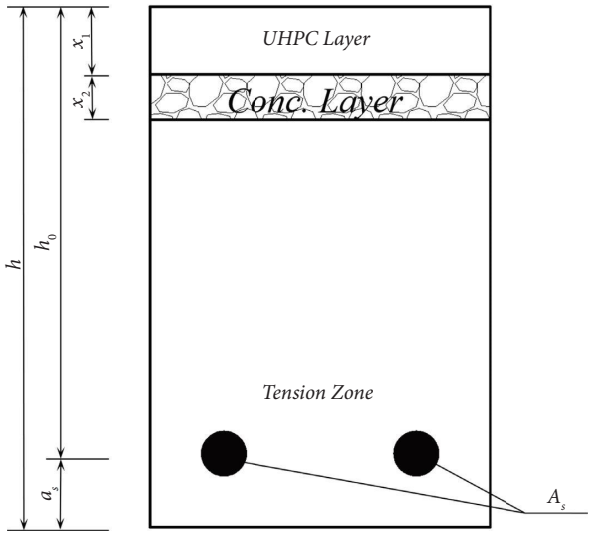

Figure 13: Proposed section of UB30-22-24.

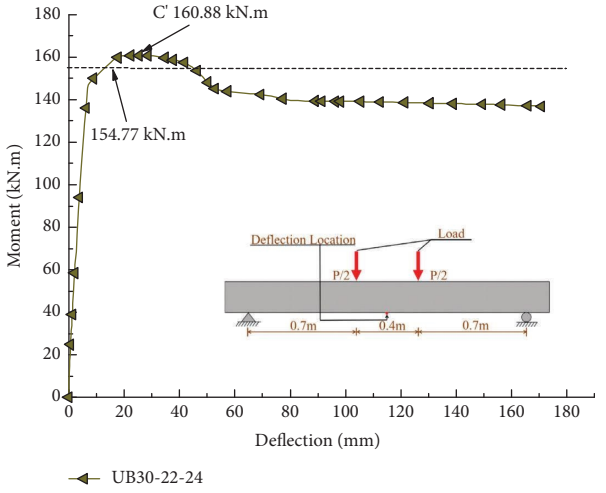

Figure 14: Comparison of results between finite element model and prediction model.

compression zone; f_c is the design value of axial compressive strength of concrete; b is the cross-section width; h_0 is the effective height of the section; x is the height of concrete compression zone; f_y is the yield strength of rebar; A_s is sectional area of tension rebar.

$$\alpha_1 f_{cUHPC} b x_1 + \alpha_2 f_c b x_2 = f_y A_s, \tag{7}$$

$$M_u = \alpha_1 f_{cUHPC} b x_1 \left(h_0 - \frac{x_1}{2}\right) + \alpha_2 f_c b x_2 \left(h_0 - x_1 - \frac{x_2}{2}\right). \tag{8}$$

For UB-2, ultimate flexural bearing capacity can be predicted by Formula (6). Since there are two types of materials in the compression zone of UB-2, it is necessary to revise Formulas (5) and (6) to obtain Formulas (7) and (8).

Among them, $\alpha_1 = \alpha_2 = 1$; $f_{cUHPC} = 144.82$ MPa; $b = 150$ mm; $x_1 = 30$ mm; $h_0 = 199$ mm; $f_c = 24.0$ MPa; $x^2 = 73.1$ mm; $f_y = 405$ MPa; $A_s = 759.88$ mm^2; as = 31 mm.

According to formula (8), ultimate flexural moment of UB30-22-24 is 154.77 kN.m, and the result of the finite element model is 160.88 kN.m. The result of the finite element model is 3.95% larger than that of the experiment, which are close to each other, indicating the correctness of the prediction model, as shown in Figure 14.

4. Conclusions

A new structural form of UHPC layer reinforced over-reinforced beams is proposed, and its effectiveness in improving flexural bearing capacity and ductility of over-reinforced beams is discussed.

(1) The finite element model was used to simulate the whole loading process of CB-2, and its load-deflection curve, flexural bearing capacity, and failure state were highly consistent with the experimental results, which verified the correctness of finite element model.

(2) The flexural bearing capacity and ductility of RC beams will be significantly improved by adding UHPC layer in the compression zone of over-reinforced beams.

(3) Increasing the thickness of UHPC layer or using a larger area of longitudinal tension rebar will increase flexural bearing capacity of RC beams, but deflection ductility coefficient will decrease accordingly. The change in concrete strength has little influence on flexural bearing capacity of RC beams, while the ductility of RC beams will be reduced when using higher strength concrete.

(4) A prediction model for flexural bearing capacity of UHPC reinforced over-reinforced beams is proposed, which is in good agreement with the results of the finite element model.

Data Availability

The data used to support the findings of this study are available from the corresponding author upon request.

Conflicts of Interest

The authors declare that they have no conflicts of interest.

Acknowledgments

This study was supported by two key funds: (1) Science and Technology Planning Project of Anyang, Henan Province, China (2022C01GX038) and (2) Science and Technology Planning Project of Henan Province, China (222102320040).

References

[1] S. Altin, O. Anil, and M. E. Kara, "Improving shear capacity of existing RC beams using external bonding of steel plates," *Engineering Structures*, vol. 27, no. 5, pp. 781–791, 2005.

[2] H. Rahimi and A. Hutchinson, "Concrete beams strengthened with externally bonded FRP plates," *Journal of Composites for Construction*, vol. 5, no. 1, pp. 44–56, 2001.

[3] T. H. K. Kang, J. Howell, S. Kim, and D. J. Lee, "A state-of-the-art review on debonding failures of FRP laminates externally adhered to concrete," *International Journal of Concrete Structures and Materials*, vol. 6, no. 2, pp. 123–134, 2012.

[4] N. M. Azmee and N. Shafiq, "Ultra-high performance concrete: from fundamental to applications," *Case Studies in Construction Materials*, vol. 9, Article ID e00197, 2018.

[5] B. Graybeal, *Ultra-High Performance Concrete*, Federal Highway Administration, McLean, VA, 2011.

[6] B. Graybeal, *Material Property Characterization of Ultra-high Performance Concrete*, Federal Highway Administration, McLean, VA, 2006.

[7] P. R. Prem, A. Ramachandra Murthy, G. Ramesh, B. H. Bharatkumar, and N. R. Iyer, "Flexural behaviour of damaged RC beams strengthened with ultra high performance concrete," *Advances in Structural Engineering*, vol. 89, pp. 2057–2069, 2015.

[8] B. Graybeal, *UHPC in the U.S. Highway Infrastructure*, Federal Highway Administration, McLean, VA, 2009.

[9] M. Zhou, W. Lu, J. W. Song, and G. C. Lee, "Application of ultra-high performance concrete in bridge engineering," *Construction and Building Materials*, vol. 186, pp. 1256–1267, 2018.

[10] K. H. Khayat and M. Valipour, *Design of Ultra High Performance Concrete as an Overlay in Pavements and Bridge Decks*, Missouri University of Science and Technology, Center for Transportation Infrastructure and Safety, Missouri, 2014.

[11] R. Bugers, J. Walraven, G. A. Plizzari, and G. Tiberti, *Structural behavior of SFRC tunnel segments during TBM operations*, pp. 1461–1467, World Tunnel Congress ITA-AITES 2007, Prague, Czech Republic, 2007.

[12] H. Yin, W. Teo, and K. Shirai, "Experimental investigation on the behaviour of reinforced concrete slabs strengthened with ultra-high performance concrete," *Construction and Building Materials*, vol. 155, pp. 463–474, 2017.

[13] C. Oesterlee, *Structural Response of Reinforced UHPFRC and RC Composite Members"*, Doctoral thesis of Swiss federal Institute of Technology in Lausanne, Lausanne, 2010.

[14] M. Farzad, *Retrofitting of Bridge Elements Subjected to Predominantly Axial Load Using UHPC Shell"*, Doctoral thesis of Florida International University, Miami, 2019.

[15] A. Ramachandra Murthy, B. Karihaloo, P. Vindhya Rani, and D. Shanmuga Priya, "Fatigue behaviour of damaged RC beams Strengthened with Ultra high performance fibre

Reinforced Concrete," *International Journal of Fatigue*, vol. 116, pp. 659–668, 2018.

[16] M. Slowik, *The analysis of failure in concrete and reinforced concrete beams with different reinforcement ratio"*, Archive of Applied Mechanics, vol. 89, pp. 885–895, 2018.

[17] M. N. Hadi and N. M. Elbasha, "Displacement ductility of helically confined HSC beams," *The Open Construction & Building Technology Journal*, vol. 2, no. 1, pp. 270–279, 2008.

[18] P. A. Whitehead and T. J. Ibell, "Deformability and ductility in over-reinforced concrete structures," *Magazine of Concrete Research*, vol. 56, no. 3, pp. 167–177, 2004.

[19] H. A. Mohamed, "Improvement in the ductility of over-reinforced NSC and HSC beams by confining the compression zone," *Structures*, vol. 16, pp. 129–136, 2018.

[20] Y. A. Priastiwi, I. Imran, Nuroji, and A. Hidayat, "Behavior of ductile beam with addition confinement in compression zone," *Procedia Engineering*, vol. 95, pp. 132–138, 2014.

[21] M. Fahiminia and A. Shishegaran, "Evaluation of a developed bypass viscous damper performance," *Frontiers of Structural and Civil Engineering*, vol. 14, no. 3, pp. 773–791, 2020.

[22] A. Shishegaran, H. Varaee, T. Rabczuk, and G. Shishegaran, "High correlated variables creator machine: prediction of the compressive strength of concrete," *Computers & Structures*, vol. 247, no. 247, Article ID 106479, 2021.

[23] A. Bigdeli, A. Shishegaran, M. A. Naghsh, B. Karami, A. Shishegaran, and G. Alizadeh, "Surrogate models for the prediction of damage in reinforced concrete tunnels under internal water pressure," *Journal of Zhejiang University - Science*, vol. 22, no. 8, pp. 632–656, 2021.

[24] A. Shishegaran, M. R. Ghasemi, and H. Varaee, "Performance of a novel bent-up bars system not interacting with concrete," *Frontiers of Structural and Civil Engineering*, vol. 13, no. 6, pp. 1301–1315, 2019.

[25] A. Shishegaran, B. Karami, T. Rabczuk, A. Shishegaran, M. A. Naghsh, and M. Mohammad Khani, "Performance of fixed beam without interacting bars," *Frontiers of Structural and Civil Engineering*, vol. 14, no. 5, pp. 1180–1195, 2020.

[26] A. Shishegaran, M. Moradi, M. A. Naghsh, B. Karami, and A Shishegaran, "Prediction of the load-carrying capacity of reinforced concrete connections under post-earthquake fire," *Journal of Zhejiang University - Science*, vol. 22, no. 6, pp. 441–466, 2021.

[27] Y. P. Zhu, Y. Zhang, H. H. Hussein, and G. D. Chen, "Numerical modeling for damaged reinforced concrete slab strengthened by ultra-high performance concrete (UHPC) layer," *Engineering Structures*, vol. 209, Article ID 110031, 2020.

[28] S. Q. Yuan, Z. Liu, and T. Tong, "Investigation of over-nonlocal damage and interface cohesive models for simulating structural behaviors of composite UHPC-NC members," *Structures*, vol. 28, pp. 2617–2632, 2020.

[29] M. K. Deng, M. Zhang, F. D. Ma, F. Y. Li, and H. Z. Sun, "Flexural strengthening of over-reinforced concrete beams with highly ductile fiber-reinforced concrete layer," *Engineering Structures*, vol. 231, Article ID 111725, 2021.

[30] L. Liu and S. Wan, "Flexural bearing capacity of reinforced concrete beams reinforced with carbon fiber reinforced plastics strips and ultra-high performance concrete layers," *International Journal of Building Pathology and Adaptation*, 2022.

[31] L. Liu, X. Ma, L. Yan, and Y. Wang, "An innovative reinforcement method: the combination of CFRP bars and UHPC layer is applied to the flexural reinforcement of RC beams," *Multidiscipline Modeling in Materials and Structures*, vol. 18, no. 2, pp. 308–327, 2022.

[32] Chinese National Standards, *Code for Design of Steel Structures GB 50017-2003*, Chinese Standard Press, Beijing, 2003.

[33] J. G. Nie and Y. H. Wang, "Comparison study of constitutive model of concrete in ABAQUS for static analysis of structures," *Engineering Mechanics*, vol. 30, no. 4, pp. 59–67, 2013.

[34] S. H. Lee, A. Abolmaali, K. J. Shin, and H. D. Lee, "ABAQUS modeling for post-tensioned reinforced concrete beams," *Journal of Building Engineering*, vol. 30, Article ID 101273, 2020.

[35] ABAQUS, *ABAQUS Analysis User's Manual Version 6.13*, Assault Systems, Dassault Systems Simulia Corporation, Rhode Island, USA, 2013.

[36] A. Raza, Q. U. Z. Khan, and A. Ahmad, "Numerical investigation of load-carrying capacity of GFRP-reinforced rectangular concrete members using CDP model in ABAQUS," *Advances in Civil Engineering*, vol. 2019, pp. 1745341–1745421, 2019.

[37] Chinese National Standards, *Code for Design of Concrete Structures GB 50010-2010*, China Building Industry Press, Beijing, 2015.

[38] Z. Zhang, X. D. Shao, W. G. Li, P. Zhu, and H. Chen, "Axial tensile behavior test of ultra high performance concrete," *China Journal of Highway and Transport*, vol. 28, no. 8, pp. 50–58, 2015.

[39] P. R. Prem, A. Ramachandra Murthy, and B. H. Bharatkumar, "Influence of curing regime and steel fibres on the mechanical properties of UHPC," *Magazine of Concrete Research*, vol. 67, no. 18, pp. 988–1002, 2015.

[40] American Association of State Highway and Transportation Officials, *Load and Resistance Factor Design (AASHTO. LRFD) (2017), Bridge Design Specifications*, 8th Ed edition.

[41] American Concrete Institute (ACI), *Building code requirements for structural concrete and commentary*, ACI 318R–11, Farmington Hills, MI, USA, 2011.

[42] K. Park, H. Choi, and G. H. Paulino, "Assessment of cohesive traction-separation relationships in ABAQUS: a comparative study," *Mechanics Research Communications*, vol. 78, pp. 71–78, 2016.

[43] D. W. Spring and G. H. Paulino, "A growing library of three-dimensional cohesive elements for use in ABAQUS," *Engineering Fracture Mechanics*, vol. 126, pp. 190–216, 2014.

[44] P. Feng, H. L. Qing, and L. P. Ye, "Discussion and definition on yield points of materials, members and structures," *Engineering Mechanics*, vol. 34, no. 3, pp. 36–46, 2017.